Aerosol trace metal fractional solubility and chemical composition of marine aerosols at the CVAO

Khanneh Wadinga Fomba, Konrad Müller and Hartmut Herrmann
Leibniz-Institute for Tropospheric Research, Leipzig, Germany
Email: fomba@tropos.de

Introduction

Fig. 1. *Cape Verde Atmospheric Observatory (CVAO) with a 30 m-tower for aerosol particle sampling , ~100 m offshore.*

The atmosphere and ocean interact in various ways that significantly affect the local and global climate. Mineral dust deposition onto the oceans plays a vital role as it provides key nutrients to the ocean biota and thereby influences the oceanic biogeochemical cycle and thus oceanic emissions.
In this work we present chemical and trace metal composition of marine aerosol at the Cape Verde Atmospheric Observatory (CVAO, Fig 1) obtained during periods of and without Saharan dust storms. The measurements were performed during intensive field studies lasting 4 – 6 weeks and also through out the year.

Experiment and Sampling

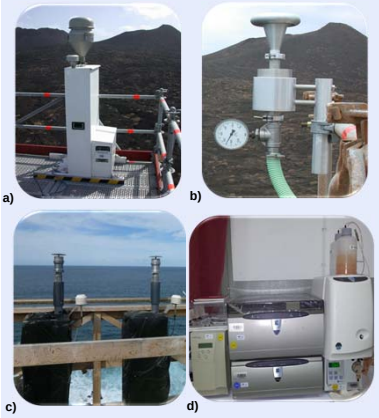

Fig. 2. *a) DIGITEL DHA-80 high volume sampler with PM_{10}-inlet, 500 l min^{-1} sampling rate b) 5-stage BERNER impactor with 75 l/min, sampling rate, stage cut-offs: 0.05 - 0.14 - 0.42 - 1.2 - 3.5 -10 µm. c) Derenda low volume sampler with PM_{10}-inlet, 4 m^3/h sampling rate d) Dionex IC with post column derivatisation*

Aerosol particles were collected at the top of a 30 m tower. PM10 samples were collected using a high volume DIGITEL DHA-80 (Fig 2a) on Quartz fiber filters continuously through out the year.

During intensive field studies, PM10 size-resolved samples were collected using a five-stage BERNER impactor (Fig. 2b) with PM_{10} cutoff 0.05-10 µm on aluminum and nuclepore foils in a daily routine. The nuclepore foils were used for total trace metal analysis using a Total Reflection X-ray fluorescence (TXRF) technique.

A low volume PM_{10} sampler (Fig. 2c) was operated every 24 h on 47 mm Teflon coated quartz filters. The filters were leached in DI water (pH 5.5), acetate buffer (pH 4.5), and HCl solutions (pH 2 and 3) via shaking for 2 hours and were analyzed with a Dionex IC (Fig. 2d) using a post column derivatization method for water soluble metals including Fe (III), Fe (II), Cu (II), Zn (II) and Mn (II)

Results

Clear differences are observed between high dust period and low dust period in the aerosol particle chemical composition. Ions made up more than 90% of the aerosol mass during low dust period and only about 12% during high dust period with sea salt ions making up most of the mass.

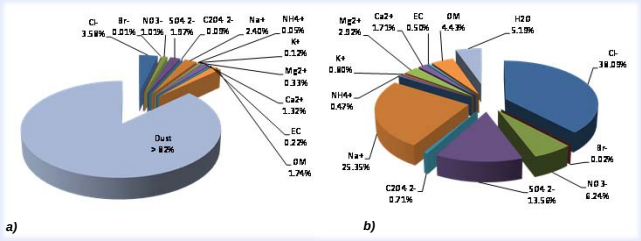

Fig. 3. *Average aerosol chemical composition observed at CVAO from 2007 to 2011 for periods of a) high dust or Saharan dust storms* ***b)****low dust or maritime air mass inflow at CVAO.*

Strong seasonal and yearly trends were observed for some of the aerosol components.

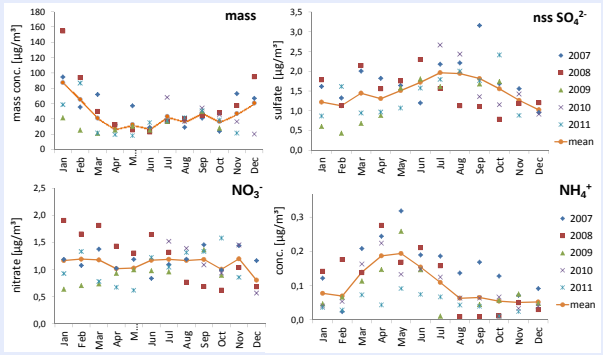

Fig. 4). *Monthly mean, seasonal and annual variation of PM10 mass concentration, non-sea-salt sulfate, nitrate, and ammonium during the five years of investigations.*

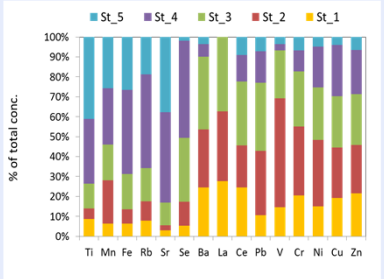

Fig. 5. *Size resolved trace metal concentration during low dust period*

Fig. 5 shows size resolved trace metal concentrations under remote conditions with Fe, Ti, Mn, Rb, Sr, mostly found in coarse mode while Se, Ba, La, Ce, Pb, V, Cr, Ni, Cu and Zn were found in the fine mode.

During dust period, Fe and Ti were found to be ideal tracers for Saharan dust. They show good correlations with other metals such as Cr, Mn, V, confirming their common source, Fig 6.

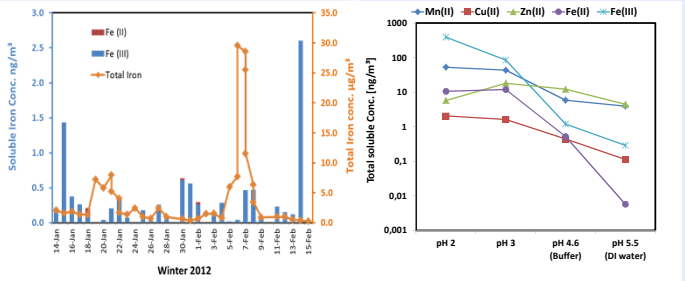

Fig. 7: *a)Total and soluble iron concentrations showing lower iron solubility during dust events and b) increase in trace metal solubility with pH*

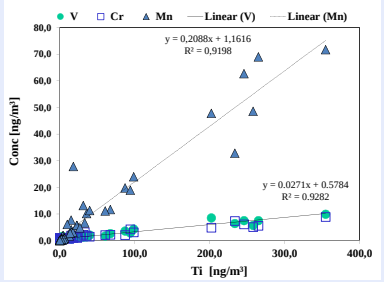

Fig. 6. *Ti showed good correlation with other metals confirming common origin..*

Soluble iron was predominantly observed in the Fe (III) state Fig 7a) and together with other metals showed a significant increase in solubility with decreasing pH (Fig 7b).

The total iron concentrations showed a reciprocal relation with water soluble iron concentrations at higher pH values but changed to a linear behavior at lower pH as shown on Fig. 8.

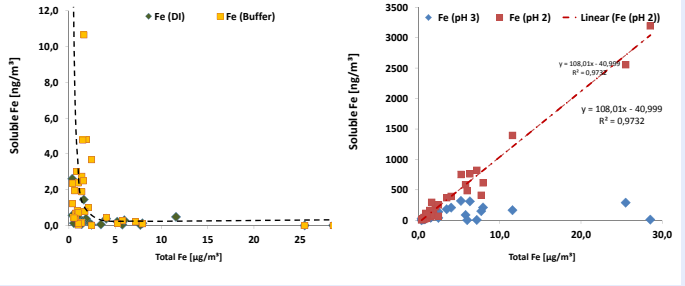

Fig. 8. *Soluble and total iron behavior at different pH*

References

Müller, K. et al., *Atmos. Chem. Phys.*, **2010,** 10,1-13.
Fomba, K. W. et al., *Atmos. Chem. Phys,* **2013**, 13,1-14.

Acknowledgement

This work was supported by the German Federal Ministry of Education and Research (BMBF) within the SOPRAN 1 and 2 projects under project numbers 03F0462J and 03F0611J, respectively.